THE JOURNAL OF PHYSICAL CHEMISTRY Letters

Letter

pubs.acs.org/JPCL

Analysis of the Origin of Open Circuit Voltage in Dye Solar Cells

Sonia R. Raga,* Eva M. Barea, and Francisco Fabregat-Santiago*

Photovoltaics and Optoelectronic Devices Group, Departament de Física, Universitat Jaume I, 12071 Castelló, Spain

ABSTRACT: Changes in the composition of the electrolyte are known to affect the parameters that determine the performance of dye solar cells. This paper describes a robust method for the analysis of the photovoltage in dye solar cells. The method focuses on the study of recombination resistance and chemical capacitance of TiO_2 obtained from impedance spectroscopy. Four dye solar cells with electrolytes producing known effects on photovoltage behavior have been studied. Effects of conduction band shifts and changes in recombination rate in the photovoltage have been evaluated quantitatively.

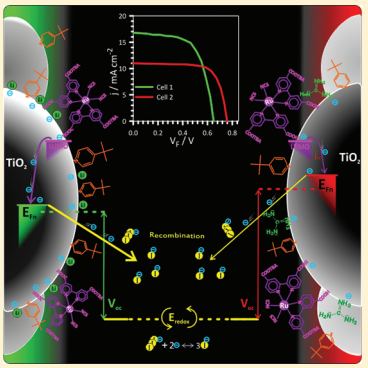

SECTION: Energy Conversion and Storage; Energy and Charge Transport

Dye-sensitized solar cells (DSCs) have attracted significant attention as alternatives to conventional solid-state photovoltaic devices during past decades.[1] This technology is suggested to be produced at a lower cost than silicon-based solar cells thanks to the easy manufacturing procedures and low temperatures used in its fabrication. DSC performance has reached power conversion efficiencies exceeding 12%.[2,3]

The operation of DSCs may be summarized as follows: Under illumination, a dye attached to a nanostructured semiconductor (generally TiO_2) absorbs a photon. This photon excites one electron from the highest occupied molecular orbital (HOMO) level into the lowest unoccupied molecular orbital (LUMO). The electron is injected from the LUMO of the dye to the conduction band (CB). Simultaneously, the oxidized dye is regenerated by a redox couple present in an electrolyte surrounding the semiconductor. Once the charges are separated between the semiconductor and electrolyte media, they can diffuse toward the contacts where they are collected.

The parameters determining DSCs solar to power conversion are the short circuit current density (j_{sc}), the open circuit photovoltage (V_{oc}) and the fill factor (FF). j_{sc} is given by the light harvesting efficiency of the dye, its capacity to inject electrons into the TiO_2 CB, and the ability of the semiconductor to transport them to the collecting electrode. V_{oc} is given by the difference of the Fermi level of electrons in the TiO_2 and the redox potential of the electrolyte, $V_{oc} = (E_{Fn} - E_{redox})/q$.[4] Finally, FF provides the reduction of the real power with respect to the product $j_{sc} \times V_{oc}$. FF is controlled mainly by total series resistance of the DSC, although it also has some contribution from recombination resistance.[5,6]

At the current stage of DSC development, the photocurrent is only limited by the absorption spectra of the dye, as most top class laboratories are able to collect nearly 100% of photogenerated electrons. Contributions of series resistance have been also reduced to a minimum through the right design of cell geometries and choice of materials. These improvements together with the use of small area samples provide large and reproducible FFs. In this scenario, the decisive parameter to enhance the performance of DSC is the open circuit photovoltage.

The maximum theoretical V_{oc} attainable by a solar cell is limited by the gap of the absorber. In the case of DSC, the effective gap of the dyes attached to TiO_2 lies around 1.60 eV.[7,8] However, best cells rarely reach V_{oc} values larger than half of this value. The main losses reducing photovoltage from its theoretical limit are the energy mismatches between E_{redox} and HOMO levels and between the E_c of the semiconductor and the LUMO of the dye, which reduce the maximum attainable voltage to $(E_c - E_{redox})/q$, and the electron recombination in the semiconductor film that determines the final E_{Fn} position.[9,10]

The purpose of this work is to deepen the understanding of the relationship between recombination losses and V_{oc}. With this aim, impedance spectroscopy (IS) was used to accurately evaluate the effects of changes in electrolyte composition over charge recombination in TiO_2. A new procedure to analyze the origin of V_{oc} is proposed. This procedure allows separating the effects of TiO_2 CB shifts and recombination rate variations in photovoltage.[10,11]

To fulfill this objective, the V_{oc} was tuned by adding electrolyte additives such as LiI, 4-*tert*-butylpyridine (tBP), 1-butyl-3-methylimidazolium iodide (BMII), and guanidinium thiocyanate (GuSCN), whose effect on the photovoltage is

Received: May 2, 2012
Accepted: June 1, 2012

   dx.doi.org/10.1021/jz3005464 | *J. Phys. Chem. Lett.* 2012, 3, 1629−1634

well-known. The electrolyte composition is shown in Table 1, and a description of the role of each of these additives follows.

Table 1. Composition of Electrolytes Employed in the Fabrication of DSCs[a]

electrolyte/DSC name	BMII	I_2	GuSCN	LiI	tBP	solvent
A	0.6 M	0.03 M	0.1 M		0.5 M	A/V (85:15)
B		0.05 M		0.5 M	0.5 M	MPN
C		0.05 M		0.5 M		MPN
D	0.6 M	0.03 M	0.1 M		0.5 M	MPN

[a]Abbreviations of the additives are as follows: BMII for 1-butyl-3-methylimidazolium iodide, GuSCN for guanidinium thiocyanate, LiI for Lithium Iodide, tBP for 4-*tert*-butylpyridine. The solvent denominations are MPN for methoxypropionitrile, and A/V for a mixture of acetonitrile and valeronitrile 85:15 in volume.

Lithium iodide is a very stable salt widely used in electrochemistry. It provides the necessary iodide anions for the redox couple in the electrolyte and the lithium cations needed to screen the negative charge in the semiconductor, and increases charge conductivity in the electrolyte. The presence of positive ions at the TiO_2 surface is known to produce a downward shift in the CB of the semiconductor, with respect to a situation in which they are not present. Previous works have reported that, the smaller the size of the cation and the larger the shift in CB, the higher the photocurrent and the lower the V_{oc}.[12,22] At long-term, the extremely small size of Li^+ allows it to intercalate into a TiO_2 lattice, degrading electron transport and recombination properties.[13] For these reasons, although convenient in this study, lithium is avoided in the fabrication of DSCs designed for long lifetimes.

tBP (Figure 1a) is reported to produce a significant upward band edge movement, thus increasing V_{oc}. This band-edge shift

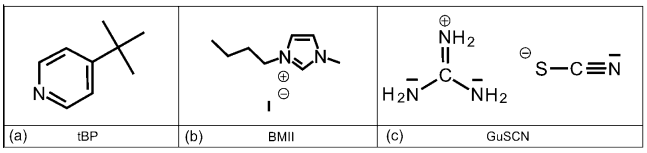

Figure 1. Molecular structures of some of the additives commonly used in DSC electrolytes: (a) tBP, (b) BMII, and (c) GuSCN. Dash on the amine group (c) stands for the nonbonding electron pair on the nitrogen atom.

is attributed to deprotonation of TiO_2 nanoparticles by amines that, together with a displacement of cations from the surface, reduces the positive charge allocated right on the semiconductor.[14] By contrast, tBP adsorbed on the semiconductor surface coats the area not covered by the dye. This fact blocks the recombination to the redox couple in the electrolyte.

Ionic liquids such as 1-butyl-3-methylimidazolium iodide (BMII) (Figure 1b) present some advantages in DSC electrolyte applications. The BMI^+ molecule is a bigger cation than Li^+ and has two amine groups in its structure. Consequently, the CB in TiO_2 remains at a higher energy than when using lithium, and the cation is not able oto intercalate into the semiconductor structure. Furthermore, BMI^+ appears to be very effective at shielding the semiconductor surface from charge recombination toward the electrolyte.[5,15]

Cations from GuSCN in Figure 1c are reported to shift downward at the TiO_2 CB around 100 mV.[17] This fact increases electron injection efficiency from the dye, enhancing photocurrent. In contrast to what is expected, GuSCN also improves V_{oc}, as the adsorption of the guanidinium cation on the TiO_2 surface produces a very effective surface passivation layer, yielding a notable decrease in recombination rate.[16,17]

In this study we also analyzed the effect of two different solvents: an acetonitrile/valeronitrile mixture and methoxypropionitrile. Acetonitrile/valeronitrile is widely used for high efficiency DSCs. The low viscosity of this solvent reduces diffusion resistance in the electrolyte, a requisite to obtain good fill factor and efficiency of the device.[5] Methoxypropionitrile is commonly chosen, as its low volatility improves long-term stability of the devices.

$j-V$ curves of DSC made with the four different electrolytes of Table 1 taken under 1 sun illumination intensity are presented in Figure 2. The photovoltaic parameters obtained from these curves are shown in Table 2.

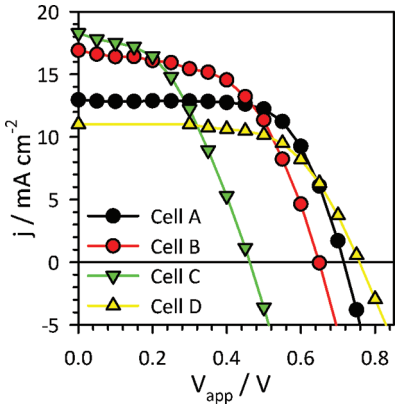

Figure 2. $j-V$ curves of the DSCs with different electrolytes as described in the text (lines) and obtained from IS measurements (symbols). The open circuit voltages differ significantly with the additives contained in the electrolyte.

Table 2. Photovoltaic Performance Parameters of DSCs Analyzed[a]

	area (cm^2)	V_{oc} (V)	J_{sc} (mA/cm^2)	FF	η (%)
cell A	0.25	0.716	12.92	0.67	6.19
cell B	0.28	0.650	16.91	0.53	5.95
cell C	0.25	0.462	18.30	0.44	3.70
cell D	0.25	0.758	11.00	0.63	5.22

[a]The name of the cells refers to the name of the electrolyte they contain given in Table 1.

Dye solar cells prepared with electrolytes A and D present similar open circuit voltage. These electrolytes only differ on the solvent, while they contain the same additives and concentrations. This result suggests that the nature of both solvents has little effect on the photovoltage. For cells B and C, the V_{oc} is much lower. These cells contain lithium iodide in the electrolyte, and neither contain ionic liquid nor GuSCN. This decrease is more pronounced for cell C, which does not contain tBP. On the other hand, cells B and C provide higher photocurrent than cells A and D.

In this first view of $j-V$ curve results, the origin of the photovoltage variation found is not conclusive, as the additives

dx.doi.org/10.1021/jz3005464 | J. Phys. Chem. Lett. 2012, 3, 1629−1634

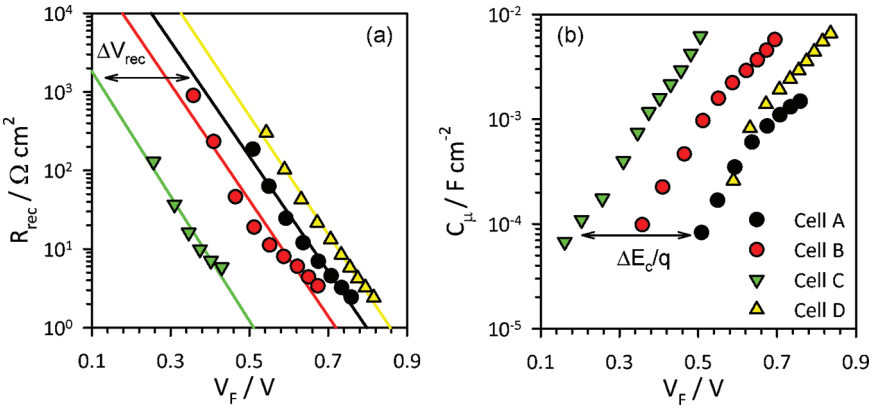

Figure 3. Impedance results of the cells with different electrolytes. (a) Recombination resistance between the semiconductor and the acceptor species in the electrolyte. (b) Chemical capacitance of the TiO_2. Voltage drop due to internal series resistance has been corrected in all plots. ΔV_{rec} and $\Delta E_c/q$ beween samples A and C are represented in panels a and b, respectively.

of the electrolytes are expected to affect both the CB energy level and recombination rates.

For a fine evaluation of the influence of the different additives used on the electrical response of the DSCs, we may use IS data. IS is a common technique that provides information about charge transport, accumulation, and loses in films and devices. Details about the interpretation of the parameters obtained through IS data in connection to the performance of DSCs are provided in recent papers.[11,18] Here we will focus in the analysis of the changes in recombination resistance (R_{rec}) and chemical capacitance (C_μ) and their relationship with the photovoltage.

Results of R_{rec} and C_μ obtained from the fitting of the Nyquist plots of the impedance spectra are shown in Figure 3. These values have been represented after subtracting the effect of the series resistance on the voltage,

$$V_F = V_{app} - V_{series} \tag{1}$$

where V_F is the corrected voltage, V_{app} is the applied voltage during the measurement, and $V_{series} = [j/(j_{sc} - j)]\int_{j_{sc}}^{j} R_{series}\, dj$ is the voltage drop at the total series resistance.[5] Main contributions to R_{series} are given by the contacts, the conducting glass, charge transfer at the Pt counter-electrode, and electrolyte diffusion resistances.

The first clear result observed in Figure 3a is the strong correlation between V_{oc} and R_{rec}: Using cell A as a reference, the voltage differences found in the V_{oc} of the samples analyzed match very well with the voltage shift in R_{rec} ($\Delta V_{R_{rec}}$) observed in Figure 3a (see Table 3). This indicates that R_{rec} is the parameter that dominates photovoltage, despite the differences in j_{sc}.

This behavior has its origin in the relationship between the resistance, the current, and the voltage given by[18]

$$R_{rec} = \left(\frac{\partial j_{rec}}{\partial V_F}\right)^{-1} \approx R_0 \exp\left[-\beta \frac{qV_F}{k_B T}\right] \tag{2}$$

where j_{rec} is the current for charge losses produced by recombination ($j = j_{sc} - j_{rec}$), β is a coefficient given by the nonlinear charge transfer ($\beta < 1$) of electrons in TiO_2 to electrolyte, q is the electron charge, k_B is Boltzmann's constant, T is the temperature, and R_0 is a parameter that determines the activation of recombination given by[18,19]

Table 3. Photovoltaic Parameters Obtained from IS Analysis[a]

parameters	Cell A	Cell B	Cell C	Cell D
average R_{series} (Ω)	15.1	15.8	22.3	27.3
R_0 (Ω cm^2)	6.82×10^5	2.05×10^5	1.13×10^4	2.87×10^6
β	0.439	0.443	0.477	0.452
α	0.282	0.308	0.349	0.259
calculated V_{oc} (V)	0.712	0.651	0.454	0.768
$E_c - E_{redox}$ (eV)	0.976	0.801	0.618	0.936
$\Delta E_c/q$ vs ref (mV)	ref.	−180	−330	−50
ΔV_k (mV)	ref.	+114	+78	+96
$\Delta V_{R_{rec}}$ (mV)	ref.	−66	−252	+44

[a] R_{series} is the series resistance of the cell; R_0 is the recombination prefactor parameter from eq 3; β is the charge transfer coefficient for recombination of electrons; α is the exponential electron trap distribution parameter; calculated V_{oc} is the open circuit voltage obtained from eq 6 at T = 305 K; $E_c - E_{redox}$ is the value estimated from eq 9, taking $N_t = 2.5 \times 10^{19}$ cm^{-3}; ΔE_c vs ref is the energy shift needed to compare all the cells at the same CB level obtained after displacing the capacitances in Figure 3b; ΔV_k is the voltage difference in R_{rec} due to the differences in recombination rates; $\Delta V_{R_{rec}}$ is the sum of $\Delta E_c/q$ and ΔV_k.

$$R_0 = \frac{\sqrt{\pi \lambda k_B T}}{q^2 L \alpha k_r c_{ox} N_s} \exp\left[\alpha \frac{E_c - E_{redox}}{k_B T} + \frac{\lambda}{4 k_B T}\right] \tag{3}$$

with L being the film thickness, c_{ox} the concentration of acceptor species (here I_3^-) in the electrolyte, λ the reorganization energy of the acceptor species, N_s the total number of surface states contributing to the recombination, α a parameter related to the electron trap distribution below the CB, and k_r the rate constant accounting for recombination kinetics.

In general, as may be observed in Figure 3a, R_{rec} approaches quite well the single exponential behavior given in eq 2. This fact together with the general approach for the $j-V$ curve in DSC[18,20]

$$j = j_{sc} - j_0(\exp[\beta q V_F / k_B T] - 1) \tag{4}$$

yields

dx.doi.org/10.1021/jz3005464 | J. Phys. Chem. Lett. 2012, 3, 1629−1634

$$j = j_{sc} + j_0 - \frac{k_B T}{\beta q}\frac{1}{R_{rec}} \quad (5)$$

where $j_0 = k_B T/\beta q R_0$ is a constant equivalent to reverse bias dark current in p−n junction diodes and solar cells. Equation 5 together with eq 2 yields, at open circuit conditions ($j = 0$),

$$V_{oc} = \frac{k_B T}{\beta q} \ln \frac{\beta q R_0 j_{sc}}{k_B T} \quad (6)$$

As may be seen in Table 3, calculation of open circuit photovoltage using eq 6 with the values of R_0 and β extracted from Figure 3a fit well (within 10 mV error) with the values obtained from the $j-V$ curve in Table 2. Therefore, once the photocurrent is known, eq 6 allows calculating V_{oc} exclusively from recombination parameters. Note that this expression is very close to others generally used in the literature but using direct experimental parameters obtained from IS.[9]

A quick look to eq 6 and Tables 2 and 3 suggests that, as β is similar in all the samples, and the changes in the value of j_{sc} only may produce small modifications in the logarithm calculation, the main element determining the differences in V_{oc} is the prefactor R_0 of the recombination resistance. This assumption agrees well with the results commented above.

To complete this analysis, the origin of the observed differences in R_{rec} was investigated. Equation 3 shows the dependence of R_0 (and then V_{oc}) on both the energy difference $E_c - E_{redox}$ and the rate k_r at which the electrons in TiO_2 are lost. Quantification of the contribution of each of these effects to the voltage is feasible with data obtained from IS. First, it is needed to have an estimation of the position of the CB, or at least of its shift (ΔE_c) with respect to a reference (cell A in our case). Then, using the definition of the voltage at the equivalent CB position,[18]

$$V_{ecb} = V_F - \Delta E_c/q \quad (7)$$

it will be possible to compare all the samples at a voltage in which the TiO_2 contains the same electron concentration.

The chemical capacitance, C_μ, represented in Figure 3b, provides quantitative information about the position of the CB as[21]

$$C_\mu = C_0 \exp[\alpha q V_F/k_B T] \quad (8)$$

with

$$C_0 = L(1-p)\alpha\frac{q^2 N_t}{k_B T} \exp[\alpha(E_{redox} - E_c)/k_B T] \quad (9)$$

being a constant, N_t the total number of trap states below the CB, and p the porosity of the film. Provided that all the films have the same geometrical dimensions and assuming that the additives do not change the number of traps in the TiO_2, shifts in the capacitance of Figure 3b are equivalent to shifts in E_c. This procedure was used to calculate the ΔE_c shown in Table 3, which, within experimental error, matches quite well with the changes in $E_c - E_{redox}$ obtained from eq 9. In Figure 4 one can see the collapse of the capacitance of all the samples in the representation at V_{ecb}.

The data in Table 3 and Figure 3b show the different displacement of the CB toward lower energies for samples B, C, and D with respect to sample A. The small difference found for samples A and D indicates that the change in solvent has a minor role in changing the CB. By contrast, and according to expectations, for sample B, the use of LiI instead of BMII and GuSCN results in a large downward shift in CB, which is even greater for the sample with electrolyte C in which tBP is not present.

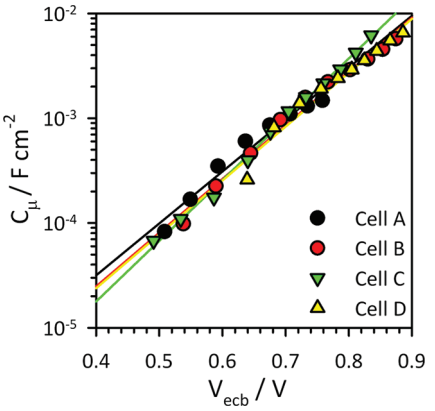

Figure 4. Chemical capacitance represented at the same energy level of the CB, taking cell A as a reference.

The values of $\Delta E_c/q$ and ΔV_{oc} do not match; otherwise when $j-V$ curves were compared at V_{ecb} as in Figure 5a, the displaced V_{oc} would match for all the samples. This result suggests that changes in the rate transfer due to the variations in electrolyte composition produce relevant effects in the photopotential. The relative value of this contribution, labeled ΔV_k in Table 3, may be obtained measuring the voltage difference between R_{rec} of the different samples in Figure 5b. As this representation of R_{rec} is free from the effect of CB shifts, ΔV_k computes the voltage contribution of recombination kinetics to the V_{oc} for the different cells. Therefore it is possible to calculate the contribution to the photovoltage due to changes in the rate constant, despite the fact that absolute values of k_r could not be estimated as the value of N_s is not known.

It was found that ΔV_k takes values very close to the differences in the displaced V_{oc} of Figure 5(a). As may be seen from Table 3, the sum of ΔV_k and $\Delta E_c/q$ represents the main contributions to photovoltage.

The values obtained for ΔV_k fit well with the expected effect of the electrolytes in the properties of the cells.[14−17] Thus when comparing the samples with the same solvent at V_{ecb}, it is found that cell C presents the lower R_{rec} (and lower ΔV_k) of the three. This agrees with the fact that this electrolyte has no surface blocking additives that would yield a larger k_r and smaller R_0. In the case of the sample with electrolyte B, the addition of tBP displaces the V_{oc} 18 mV upward. The extra addition of BMII and GuSCN in electrolyte D adds another 20 mV to the photovoltage with respect to sample B.

Focusing on samples A and D with the same additives but different solvents, it is observed that cell A presents a higher internal recombination that diminishes the displaced V_{oc} in 96 mV with regard to cell D. This result suggests that the passivation of the surface of TiO_2 with GuSCN and tBP is more efficient in the MPN-based electrolyte.

Finally, a small contribution to the V_{oc} has its origin in the differences of photocurrent obtained for the different cells. Thus, for a given R_{rec}, the larger photocurrent pushes the $j-V$ curve upward, yielding an increase in V_{oc}.[11] However, and as indicated above, in general, photocurrent contribution to photovoltage is small, as it is governed by eq 6.

dx.doi.org/10.1021/jz3005464 | J. Phys. Chem. Lett. 2012, 3, 1629−1634

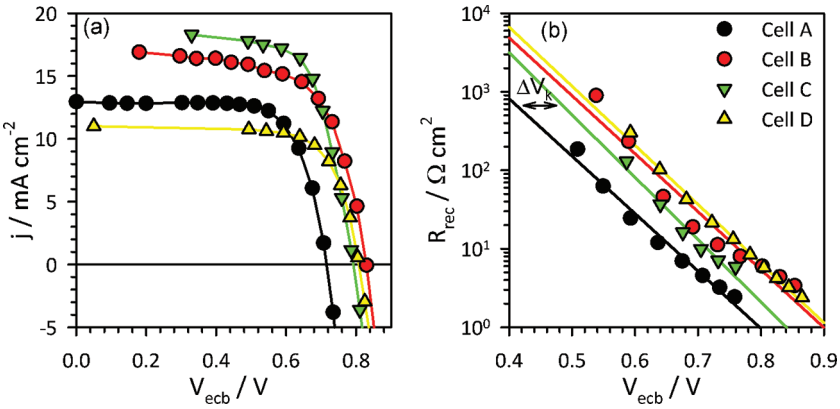

Figure 5. Values of $j-V$ curves (a) and recombination resistance (b) represented at the equivalent CB position taking cell A as a reference. In panel b, the potential shift ΔV_k between cells A and C is plotted.

The explanation of the differences between the photocurrent of the different samples fits well with the one done in previous works: The downward shift of E_c in the semiconductor leads to an enhancement of the electron injection efficiency from the dye to the TiO_2. The higher the distance between the LUMO level of the excited dye and the CB of TiO_2, the more favorable the charge transfer.[22−24] A maximum is found when all the light harvested by the dye is collected.

In summary, it has been shown that photovoltage in solar cells can be exclusively described in terms of short circuit photocurrent and recombination resistance. The method proposed here for the analysis of the data allowed evaluating the influence of CB shifts, recombination rate changes, and short circuit photocurrent in the photovoltage. In the cases presented here, changes in both CB and rate constants for recombination dominated the V_{oc}. Potentially, the procedure may be applied in the analysis of other solar cell technologies.

EXPERIMENTAL SECTION

DSC Preparation. Working electrodes for the DSC were prepared on a 15 Ω/□ FTO glass previously cleaned. A 150 nm compact TiO_2 layer was deposited by spray-pyrolisis technique with a solution of ethanol/acetil acetone/titanium-(IV) isopropoxide (3:3:2 weight ratio) and a 450 °C hot plate. The substrates were coated by doctor blade technique with a 7 μm layer of 20 nm TiO_2 nanoparticles and a 3 μm scatter layer of 450 nm TiO_2 nanoparticles (respectively 18-NRT and WER0-4 from Dyesol), and calcined at 450 °C for 30 min. After sintering, films were immersed into 40 mM $TiCl_4$ (aq) at 70 °C for 30 min, rinsed with Milli-Q water, and sintered at 570 °C for 10 min. After cooling down to 40 °C, the TiO_2 electrodes were immersed overnight into a 0.5 mM dye solution containing Ditetrabutylammonium cis-bis-(isothiocyanato) bis(2,2′-bipyridyl-4,4′-dicarboxylato) ruthenium(II) (N719) in a mixture of acetonitrile and *tert*-butanol 1:1 volume ratio.

As counter electrodes, 8 Ω/□ FTO-coated glasses were drilled with a 1 mm diameter drill tip and cleaned. Over this electrode, a drop of chloroplatinic acid solution from Sigma Aldrich was spread, and the resulting glass was fired in a 450 °C air flow.

The working and counter electrodes were assembled in a sandwich-type cell by pressing at 95 °C with a hot-melt film (Surlyn 25 μm thickness) as a sealant and spacer between electrodes. A drop of electrolyte solution was put through the drilled holes and sealed with Surlyn and 0.1 mm thick glasses. Finally, a tin contact was weld on the edge of FTO outside the cells.

The compositions of the four different electrolytes employed in this work are detailed in Table 1. The assembled solar cells were named as the type of electrolyte they contain.

Solar Cell Characterization. Acquisition of the IS measurements were carried out with a FRA-equipped PGSTAT-30 from Autolab. The amplitude of the AC signal was 25 mV at low applied voltages and 10 mV at high forward bias. The frequency range scanned values between 400 kHz and 0.1 Hz at the different V_{app}. Illumination was provided by a 1000 W class-A solar simulator from Newport, filtered at AM1.5 G and with the light intensity adjusted with an NREL-calibrated Si solar cell with a KG-5 filter to 1 sun (100 mW/cm^2). All measurements were carried out with an opaque mask 0.5 mm per side bigger than the active area.

AUTHOR INFORMATION

Corresponding Author

*E-mail: fran.fabregat@fca.uji.es.

Notes

The authors declare no competing financial interest.

ACKNOWLEDGMENTS

The authors want to thank Prof. Juan Bisquert for fruitful discussions. This work is supported by the "Institute of Nanotechnologies for Clean Energies" funded by the Generalitat Valenciana under project ISIC/2012/008, Ministerio de Economia y Competitividad of Spain under Projects Consolider HOPE CSD2007-00007 and MAT2010-19827 and Generalitat Valenciana under Project PROMETEO/2009/058. S.R.R. acknowledges financial support from the Bancaixa foundation under Project Innova 11I272.

REFERENCES

(1) O' Regan, B.; Grätzel, M. A Low-Cost High-Efficiency Solar Cell Based on Dye-Sensitized Colloidal TiO_2 Films. *Nature* **1991**, *353*, 737.

(2) Yu, Q.; Wang, Y.; Yi, Z.; Zu, N.; Zhang, J.; Zhang, M.; Wang, P. High-Efficiency Dye-Sensitized Solar Cells: The Influence of Lithium Ions on Exciton Dissociation, Charge Recombination, and Surface States. *ACS Nano* **2010**, *4*, 6032−6038.

(3) Yella, A.; Lee, H.-W.; Tsao, H. N.; Yi, C.; Chandiran, A. K.; Nazeeruddin, M. K.; Diau, E. W.-G.; Yeh, C.-Y.; Zakeeruddin, S. M.; Grätzel, M. Porphyrin-Sensitized Solar Cells with Cobalt (II/III)

Based Redox Electrolyte Exceed 12% Efficiency. *Science* **2011**, *334*, 629−634.
(4) Wang, Q.; Ito, S.; Grätzel, M.; Fabregat-Santiago, F.; Mora-Seró, I.; Bisquert, J.; Bessho, T.; Imai, H. Characteristics of High Efficiency Dye-Sensitized Solar Cells. *J. Phys. Chem. B* **2006**, *110*, 19406−19411.
(5) Fabregat-Santiago, F.; Bisquert, J.; Palomares, E.; Otero, L.; Kuang, D.; Zakeeruddin, S. M.; Grätzel, M. Correlation between Photovoltaic Performance and Impedance Spectroscopy of Dye-Sensitized Solar Cells Based on Ionic Liquids. *J. Phys. Chem. C* **2007**, *111*, 6550−6560.
(6) Chiba, Y.; Islam, A.; Watanabe, Y.; Komiya, R.; Koide, N.; Han, L. Dye-Sensitized Solar Cells with Conversion Efficiency of 11.1. *Jpn. J. Appl. Phys.* **2006**, *45*, L638−L640.
(7) Grätzel, M. Recent Advances in Sensitized Mesoscopic Solar Cells. *Acc. Chem. Res.* **2009**, *42*, 1788−1798.
(8) Bisquert, J. Dilemmas of Dye-Sensitized Solar Cells. *ChemPhysChem* **2011**, *12*, 1633−1636.
(9) Boschloo, G.; Hagfeldt, A. Characteristics of the Iodide/Triiodide Redox Mediator in Dye-Sensitized Solar Cells. *Acc. Chem. Res.* **2009**, *42*, 1819−1826.
(10) Barea, E. M.; Ortiz, J.; Payá, F. J.; Fernández-Lázaro, F.; Fabregat-Santiago, F.; Sastre-Santos, A.; Bisquert, J. Energetic Factors Governing Injection, Regeneration and Recombination in Dye Solar Cells with Phthalocyanine Sensitizers. *Energy Environ. Sci.* **2010**, *3*, 1985−1994.
(11) Barea, E. M.; Zafer, C.; Gultekin, B.; Aydin, B.; Koyuncu, S.; Icli, S.; Fabregat-Santiago, F.; Bisquert, J. Quantification of the Effects of Recombination and Injection in the Performance of Dye-Sensitized Solar Cells Based on N-Substituted Carbazole Dyes. *J. Phys. Chem. C* **2010**, *114*, 19840−19848.
(12) Pelet, S.; Moser, J.-E.; Grätzel, M. Cooperative Effect and Adsorbed Cations and Iodide on the Interception of Back Electron Transfer in the Dye Sensitization of Nanocrystalline TiO_2. *J. Phys. Chem. B* **2000**, *104*, 1791−1795.
(13) Kopidakis, N.; Benkstein, K. D.; van de Lagemaat, J.; Frank, A. J. Transport-Limited Recombination of Photocarriers in Dye-Sensitize Nanocrystalline TiO_2 Solar Cells. *J. Phys. Chem. B* **2003**, *107*, 11307.
(14) Schlichthörl, G.; Huang, S. Y.; Sprague, J.; Frank, A. J. Band Edge Movement and Recombination Kinetics in Dye-Sensitized Nanocrystalline TiO_2 Solar Cells: A Study by Intensity Modulated Photovoltage Spectroscopy. *J. Phys. Chem. B* **1997**, *101*, 8141−8155.
(15) Wang, P.; Zakeeruddin, S. M.; Humphry-Baker, R.; Grätzel, M. A Binary Ionic Liquid Electrolyte to Achieve 7% Power Conversion Efficiencies in Dye-Sensitized Solar Cells. *Chem. Mater.* **2004**, *16*, 2694−2696.
(16) Zhang, Z.; Zakeeruddin, S. M.; O'Regan, B. C.; Humphry-Baker, R.; Grätzel, M. Influence of 4-Guanidinobutyric Acid as Coadsorbent in Reducing Recombination in Dye-Sensitized Solar Cells. *J. Phys. Chem. B* **2005**, *109*, 21818−21824.
(17) Kopidakis, N.; Neale, N. R.; Frank, A. J. Effect of an Adsorbent on Recombination and Band-Edge Movement in Dye-Sensitized TiO_2 Solar Cells: Evidence for Surface Passivation. *J. Phys. Chem. B* **2006**, *110*, 12485−12489.
(18) Fabregat-Santiago, F.; Garcia-Belmonte, G.; Mora-Sero, I.; Bisquert, J. Characterization of Nanostructured Hybrid and Organic Solar Cells by Impedance Spectroscopy. *Phys. Chem. Chem. Phys.* **2011**, *13*, 9083−9118.
(19) Bisquert, J.; Fabregat-Santiago, F. Impedance Spectroscopy: A General Introduction and Application to Dye-Sensitized Solar Cells. In *Dye-Sensitized Solar Cells*; Kalyanasundaram, K., Ed.; EPFL Press and CRC Press: Lausanne, Switzerland and Boca Raton, FL, 2010.
(20) Sze, S. M. *Physics of Semiconductor Devices*, 2nd ed.; John Wiley and Sons: New York, 1981.
(21) Bisquert, J. Chemical Capacitance of Nanostructured Semiconductors: Its Origin and Significance for Heterogeneous Solar Cells. *Phys. Chem. Chem. Phys.* **2003**, *5*, 5360.
(22) Liu, Y.; Hagfeldt, A.; Xiao, X.-R.; Lindquist, S.-E. Investigation of Influence of Redox Species on the Interfacial Energetics of a Dye Sensitized Nanoporous TiO_2 Solar Cell. *Sol. Energy Mater. Sol. Cells* **1998**, *55*, 267−281.
(23) van de Lagemaat, J.; Park, N.-G.; Frank, A. J. Influence of Electrical Potential Distribution, Charge Transport, and Recombination on the Photopotential and Photocurrent Conversion Efficiency of Dye-Sensitized Nanocrystalline TiO_2 Solar Cells: A Study by Electrical Impedance and Optical Modulation Techniques. *J. Phys. Chem. B* **2000**, *104*, 2044−2052.
(24) Fabregat-Santiago, F.; Bisquert, J.; Garcia-Belmonte, G.; Boschloo, G.; Hagfeldt, A. Impedance Spectroscopy Study of the Influence of Electrolyte Conditions in Parameters of Transport and Recombination in Dye-Sensitized Solar Cells. *Sol. Energy Mater. Sol. Cells* **2005**, *87*, 117−131.